Hindawi Publishing Corporation
Journal of Spectroscopy
Volume 2015, Article ID 450485, 6 pages
http://dx.doi.org/10.1155/2015/450485

Research Article

Hydrothermal Synthesis and Structural Characterization of NiO/SnO_2 Composites and Hydrogen Sensing Properties

Chao Wei,[1] Bin Bo,[1] Fengbo Tao,[1] Yuncai Lu,[1] Shudi Peng,[2] Wei Song,[2] and Qu Zhou[3]

[1] *Jiangsu Electric Power Company Research Institute, Nanjing 211103, China*
[2] *Chongqing Electric Power Research Institute, Chongqing 401123, China*
[3] *College of Engineering and Technology, Southwest University, Chongqing 400715, China*

Correspondence should be addressed to Qu Zhou; zhouqu@swu.edu.cn

Received 6 August 2014; Revised 10 October 2014; Accepted 11 October 2014

Academic Editor: Wen Zeng

Pure SnO_2 and NiO doped SnO_2 nanostructures were successfully synthesized via a simple and environment-friendly hydrothermal method. X-ray powder diffraction (XRD), scanning electron microscopy (SEM), energy dispersive X-ray spectroscopy (EDS), and X-ray photoelectron spectra (XPS) were used to investigate the crystalline structures, surface morphologies and microstructures, and element components and their valences of the as-synthesized samples. Furthermore, planar chemical gas sensors based on the synthesized pure SnO_2 and NiO/SnO_2 composites were fabricated and their sensing performances to hydrogen, an important fault characteristic gas dissolved in power transformer oil, were investigated in detail. Gas sensing experiments indicate that the NiO/SnO_2 composites showed much higher gas response and lower working temperature than those of pure SnO_2, which could be ascribed to the formation of p-n heterojunctions between p-type NiO and n-type SnO_2. These results demonstrate that the as-synthesized NiO/SnO_2 composites a promising hydrogen sensing material.

1. Introduction

Larger oil-immersed power transformers are costly and important electrical apparatus in power supply system. Once faults happened on transformers, the safety and reliability of the power system would be affected and cause great damage to the national economy [1, 2]. As hydrogen gas (H_2) is one of the most important fault characteristic gases dissolved in oil-filled power transformers, we can timely and effectively acquire the running condition of power transformer through recognition and analysis of dissolved H_2 gas in oil [3, 4]. In recent years, interest in recognition of dissolved H_2 in transformer oil has been extremely simulated and a great deal of effort has been devoted to this field [5].

Currently, metal oxide semiconductor (MOS) [6], carbon nanotube [7], grapheme [8], infrared spectroscopy, and photoacoustic spectroscopy [9] have been reported for gas detection. And due to the remarkable advantages of simple fabrication technology, rapid response and recovery speed, and low maintenance cost and long service life, metal oxide SnO_2 has been proved to be the most promising sensing material for H_2 recognition [10–12]. However, there still exist some limitations needed to be further improved, for instance, higher operating temperature, lower gas response, and poor selectivity and stability. Thus, many scientific and technological efforts have been done to perfect SnO_2 sensing performances [5].

Among them three kinds of doping strategies are developed and reported, doping noble metals [6] or rare earth elements, using other n-type semiconductors such as ZnO and TiO_2 to form composites [11, 13], and forming p-n composites with p-type semiconductors [14] such as CuO and NiO. For example, Zeng et al. [6] synthesized Pd^{2+} doped SnO_2 nanostructures by the sol-gel method and investigated their gas sensing performances to hydrogen and its sensing mechanism by the first principles calculation. Tang et al. [15] prepared hollow hierarchical SnO_2-ZnO composite nanofibers by an electrospinning method and reported the SnO_2-ZnO composite nanofibers exhibited excellent methanol selectivity in the presence of ethanol, acetone, formaldehyde, ammonia,

toluene, and benzene at an operating temperature of 350°C. Hieu et al. [16] synthesized p-type NiO nanoparticles decorated n-type SnO_2 nanowires through thermal evaporation and reported that NiO-decorated SnO_2 NW sensors exhibit a significantly enhanced H_2S response with good improved response and recovery times. Shen et al. [17] synthesized NiO-SnO_2 nanofibers via electrospinning and investigated their sensing performances to ethanol with three types of sensor structures.

To the best of our knowledge, reports on the synthesis of p-NiO/n-SnO_2 composites through a simple and environment-friendly hydrothermal method and researches on their sensing properties for recognition of dissolved H_2 in transformer oil have been rare. Herein, in this study, we present sensitive H_2 sensors fabricated from p-NiO and n-SnO_2 nanostructures and measure their gas sensing performances toward H_2. Firstly, pure SnO_2 nanostructures and NiO/SnO_2 composites were synthesized by a hydrothermal method. And then the surface morphologies and structural features of the samples were characterized by X-ray powder diffraction (XRD), scanning electron microscopy (SEM), energy dispersive X-ray spectroscopy (EDS), and X-ray photoelectron spectra (XPS), respectively. Finally, chemical gas sensors were fabricated and their sensing performances toward H_2 were measured. We interestingly find that the NiO/SnO_2 composites sensor exhibits excellent H_2 sensing properties in comparison to the pure SnO_2 based sensor.

2. Experimental

2.1. Preparation of Pure SnO_2 and NiO/SnO_2 Composites. The sensing materials in this study, that is, pure SnO_2 and NiO/SnO_2 composites, were synthesized with a simple, facile, and environment-friendly hydrothermal method. All chemicals were analytical-grade reagents purchased from Beijing Chemical Reagent Co., Ltd. and used as received without any further purification. The detailed synthesis processes were represented as follows.

In a typical synthesis process of NiO/SnO_2 composites, firstly 2.0 mmol $SnCl_4{\cdot}5H_2O$, 0.10 mmol $Ni(CH_3COOH)_2{\cdot}4H_2O$, 3 mmol ammonium carbonate ($(NH_4)_2CO_3$), 0.1 g of citric acid, 30 mL absolute ethanol, and 30 mL distilled water were mixed together with intense magnetic stirring in a 100 mL capacity beaker. Then the mixed solution was transferred into a 100 mL Teflon autoclave, sealed, and heated at 180°C for 24 h in an electric furnace. After reaction, the autoclave was cooled to room temperature naturally, and the product was harvested by centrifugation, washed with distilled water and absolute ethanol four times, respectively, and dried at 80°C in air for further use [6, 18]. For comparison, pure SnO_2 nanomaterials were prepared in a similar synthesis process mentioned above except that no $Ni(CH_3COOH)_2{\cdot}4H_2O$ was added to the precursor solution.

2.2. Structural Characterization of Pure SnO_2 and NiO/SnO_2 Composites. The crystalline structures of the as-prepared samples were performed by X-ray powder diffraction (XRD, Rigaku D/Max-1200X, Japan) with Cu Kα radiation operated at 40 kV and 200 mA and a scanning rate of 0.02° s^{-1} from 20° to 80°. Surface morphologies and microstructures of the as-prepared nanostructures were observed with a Nova 400 Nano field emission scanning electron microscope (FE-SEM, FEI, Hillsboro, OR, USA) equipped with an energy dispersive X-ray spectroscopy (EDS). Element components and their valences of the powders were investigated by the X-ray photoelectron spectra (XPS) performed on an ESCLAB MKII using Al as the exciting source.

2.3. Fabrication and Measurement of Pure SnO_2 and NiO/SnO_2 Based Sensors. Planar chemical gas sensors were fabricated with screen-printing technique and the planar ceramic substrates were purchased from Beijing Elite Tech Co., Ltd., China. The planar chemical gas sensor was made up of three main components: the sensing material, the Ag-Pd interdigital electrode, and the ceramic substrate [2, 19]. The length, width, and thickness of the planar ceramic substrate were 13.4, 7, and 1 mm, respectively. And five pairs of Ag-Pd interdigital electrodes have been preplaced on the planar ceramic substrate with a width of 0.2 mm. Firstly, the as-synthesized sensing materials were mixed with absolute ethanol and distilled water in a weight ratio of 8 : 1 : 1 to form a paste, which was subsequently screen-printed onto the planar ceramic substrate to form a sensing film, and its thickness is about 50 μm [2, 19]. Then the sensing film was dried in air to remove the unwanted impurities, and a certain amount of antipollution solution was coated onto the surface of the sensing film as a protective layer. Finally, the fabricated sensor was aged in an aging test chamber at 80°C for 48 h.

Gas sensor properties of the fabricated sensors to H_2 were performed on a CGS-1TP (Chemical Gas Sensor-1 Temperature Pressure) intelligent gas sensing analysis system (Beijing Elite Tech Co., Ltd.) [2]. This gas sensing analysis system can automatically record the electrical resistance, sensitivity, and working temperature of the gas sensor as well as the humidity and temperature of environment. The gas response value of the sensor was designated as the ratio of sensor resistance in air to that in a mixture of H_2 gas and air [19, 20]. The response and recovery times were defined as the time taken by the sensor to achieve 90% of the total resistance change in the case of adsorption and desorption, respectively [21, 22]. All measurements were repeated several times to ensure the repeatability and stability of the sensor [23].

3. Results and Discussion

3.1. Structural and Morphological Characterizations. Figure 1 shows the typical XRD patterns of pure SnO_2 and NiO/SnO_2 composites. As shown in Figure 1 both the as-synthesized pure SnO_2 and NiO/SnO_2 composites samples are polycrystalline in nature. It can be clearly seen in Figure 1(a) that the prominent peaks at 26.6°, 33.9°, and 51.8°, which can be well indexed as (110), (101), and (211), respectively, and other smaller peaks well correspond to the standard spectrum of rutile SnO_2 given in the standard data file (JCPDS File number 41-1445). Similar XRD patterns are observed for the as-prepared NiO/SnO_2 composites samples as shown in Figure 1(b), and (111), (200), (220), and (311) peaks could

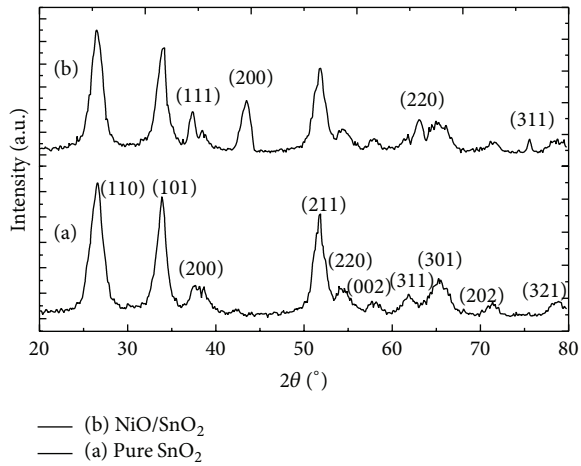

Figure 1: XRD patterns of (a) pure SnO_2 and (b) NiO/SnO_2 composites.

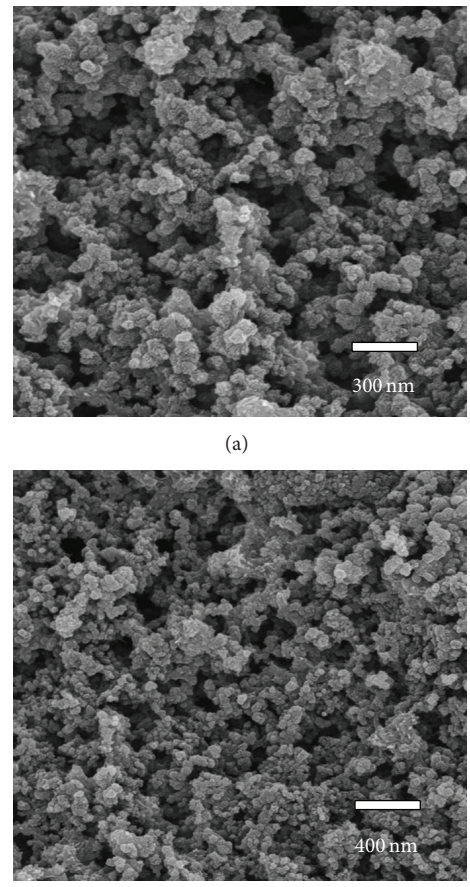

Figure 2: SEM images of (a) pure SnO_2 and (b) NiO/SnO_2 composites.

be attributed to nickel oxide. These results are consistent with other XRD characterizations reported in some similar publications [16, 17].

The surface structure and morphology characteristics of the as-synthesized samples were performed by field emission scanning electron microscopy and shown in Figure 2. As shown in Figure 2 the overview images of pure SnO_2 and NiO/SnO_2 composites nanostructures are uniform in size and shape with spherical structure. The diameters of pure SnO_2 nanostructures are ranging from 40 to 50 nm and from 38 to 46 nm for NiO/SnO_2 samples. These results indicate that in this study NiO dopant only has a slight influence on the structures and morphologies of pure SnO_2 nanostructures except for an evidently inhibitory effect on its crystalline growth.

Energy dispersive X-ray spectroscopy measurement was performed to make clear the element components of the as-synthesized samples and check whether Ni element has been successfully doped into the prepared SnO_2 nanostructures. Figure 3 is the EDS spectrum of the synthesized NiO/SnO_2 composites nanostructures, where Sn, Ni, and O element peaks are observed and the atomic ratio of Ni element to Sn element is calculated to be about 8.9 at%. Therefore, we could draw a conclusion that Ni element has been successfully incorporated into the SnO_2 nanostructures.

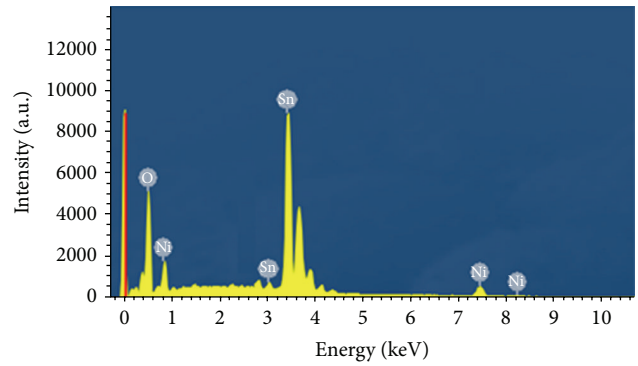

Figure 3: EDS spectrum of NiO/SnO_2 composites.

X-ray photoelectron spectra measurement was further conducted to investigate the compositions and chemical states of the elements existed in the as-prepared products. Figure 4 shows the survey spectrum of pure SnO_2 and NiO/SnO_2 composites nanostructures. As shown in Figure 4(a) only Sn and O spectra are observed and no spectrum from Ni element has been measured, while in Figure 4(b) spectra for Sn, O, and Ni element are found.

Figure 5 shows the high-resolution spectrum of Sn 3d, O 1s, and Ni 2p for the synthesized NiO/SnO_2 composites. As shown in Figures 5(a) and 5(b) the spin orbit components of the Sn $3d_{5/2}$ and Sn $3d_{3/2}$ peaks are measured at 487.1 eV and 495.4 eV, and the peak of O 1s is located at 531.9 eV, which are both well indexed to Sn^{4+} and O^{2-} in a tetragonal rutile SnO_2 structure. And in Figure 5(c) the peaks at 850.1 eV and 861.7 eV are defined as Ni $2p_{3/2}$ and Ni $2p_{1/2}$, which could be assigned to Ni^{2+} ions in the synthesized samples. Meanwhile these Ni $2p_{3/2}$ and Ni $2p_{1/2}$ peaks ruled out the existence of Ni and Ni_2O_3 in the as-prepared NiO/SnO_2 composites [24]. Based on these results, we could draw a conclusion

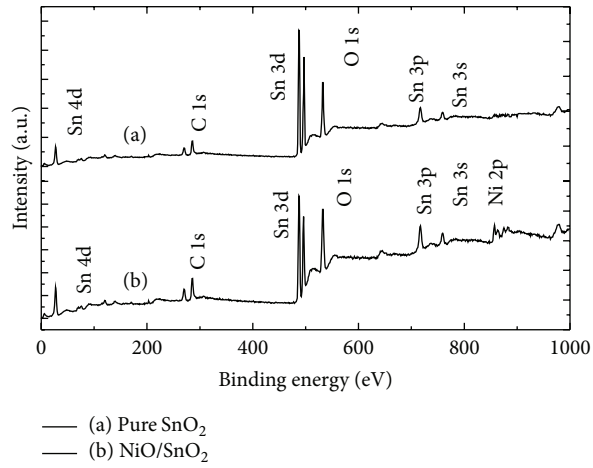

Figure 4: XPS patterns of full spectrum of (a) pure SnO_2 and (b) NiO/SnO_2 composites.

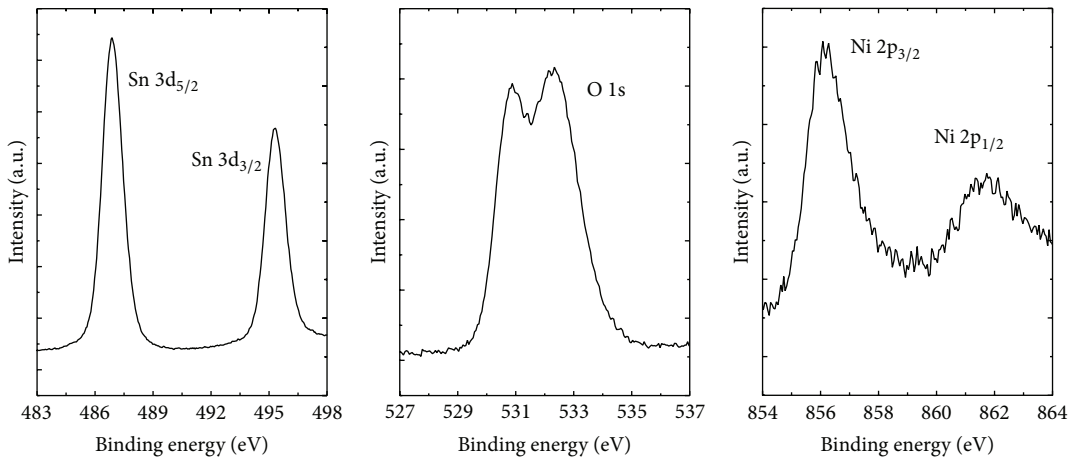

Figure 5: High-resolution spectrum of (a) Sn 3d, (b) O 1s, and (c) Ni 2p peaks.

that the synthesized samples are composed of NiO and SnO_2 nanostructures.

3.2. Gas Sensing Properties. Firstly, the sensors fabricated from the synthesized pure SnO_2 and NiO/SnO_2 composites were exposed to a certain concentration of H_2 gas at various working conditions to find out the optimum operating temperature. Figure 6 shows the gas responses of the prepared sensors to 100 μL/L of H_2 gas as a function of operating temperature ranging from 150 to 450°C. For each sensor, its gas response increases quickly firstly and obtains its maximum gas response value and then decreases rapidly with further increasing temperature. As shown in Figure 6 the optimum operating temperature of NiO/SnO_2 composites was suggested to be 325°C and 375°C for pure SnO_2 samples, where the sensor exhibits the maximum gas response value at this condition. Simultaneously, at the optimum working condition, the corresponding H_2 gas response is 45.23 for NiO/SnO_2 composites and 13.12 for pure SnO_2 samples.

Figure 7 represents the gas responses of the NiO/SnO_2 composites as a function of H_2 gas concentration with sensor working at its own optimum working condition mentioned above. Compared with pure SnO_2 samples, the NiO/SnO_2 composites sensor exhibits an obvious H_2 sensing enhancement in the whole range of concentrations. Furthermore, the gas response curve of the NiO/SnO_2 composites based sensor demonstrates a quasilinear relationship with H_2 gas concentration in the range of 1–50 μL/L. These results imply that the NiO dopant can not only increase the gas response of pure SnO_2 nanostructures but also lower its working temperature with a high linearity of 0.991 in the range of 1–50 μL/L.

A possible sensing mechanism is depicted as follows to understand the sensing behaviors of fabricated SnO_2 based gas sensors toward H_2 and get an insight into how the NiO particles improve the sensing properties of SnO_2 based sensor. As we know SnO_2 is a typical n-type semiconducting sensing material and a large number of oxygen vacancies

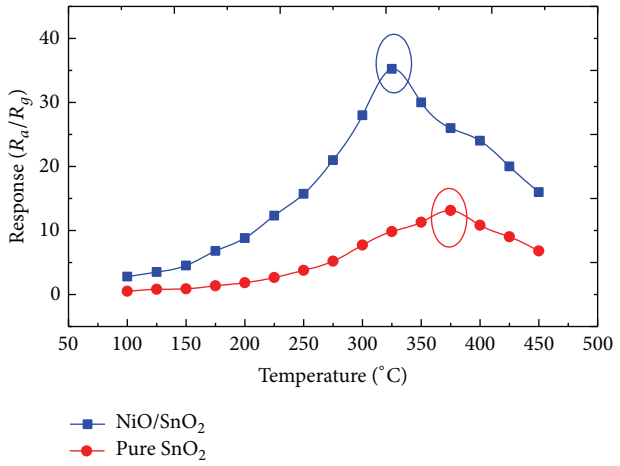

FIGURE 6: Gas responses of pure SnO_2 and NiO/SnO_2 composites based sensor to 100 μL/L of H_2 at different working temperature from 150 to 450°C.

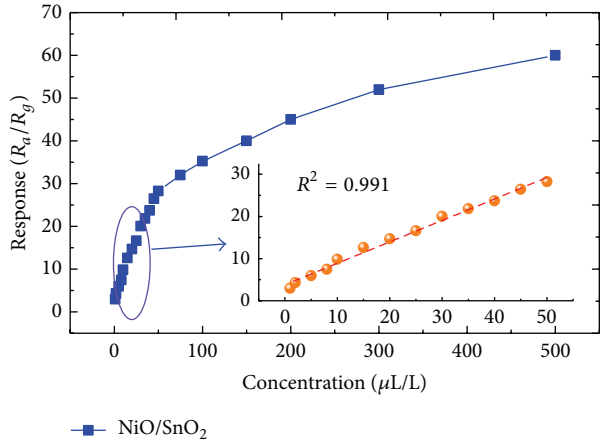

FIGURE 7: Gas responses of NiO/SnO_2 composites based sensor versus different concentration of H_2. The inset one is the linear fitting curve in the range of 1 to 50 μL/L.

exist in its crystal lattices, and its sensing behaviors are predominantly controlled by the surface resistance of sensing materials [5]. In ambient air, free oxygen molecules are absorbed on SnO_2 surface and capture electrons from the conduction band of SnO_2 to form chemisorbed oxygen ions, such as O_2^-, O^{2-}, and O^- [6]. When exposed to a reducing gas ambient (H_2 in this study), H_2 gas molecules react with chemisorbed oxygen ions. The trapped electrons are released back to the conduction band of SnO_2, resulting in an increase of the carrier concentration and electron mobility; thus a decreased resistance is measured.

The enhanced H_2 gas response and decreased working temperature of NiO/SnO_2 based sensor in the present investigation may be attributed to a p-n heterojunction effect between NiO and SnO_2 surface. A similar p-n heterojunction system has been proposed to explain the enhanced gas sensitivity of CuO-SnO_2 heterostructures to hydrogen sulfide [17, 25]. Figure 8 depicts the energy band structure

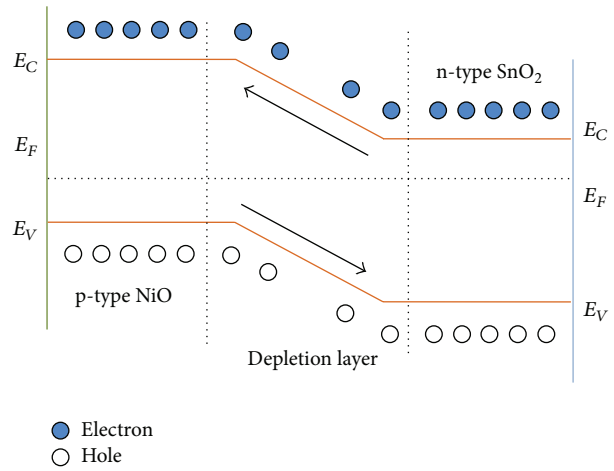

FIGURE 8: Energy band structure diagram of NiO/SnO_2 p-n heterojunction (E_C: lower level of conduction band, E_F: Fermi level, and E_V: upper level of valence band).

diagram of NiO/SnO_2 p-n heterojunction. As NiO and SnO_2 have different election affinities and work functions, a p-n heterojunction structure emerges at the surface between NiO and SnO_2, which leads to a band bending in the depletion. Then the holes transfer from oxygen-excess NiO to oxygen-deficient SnO_2 and the electrons transfer from oxygen-deficient SnO_2 to oxygen-excess NiO until the system obtains an equalization in the Fermi levels between NiO and SnO_2 [16, 17]. This process will lead to a wider depletion layer, and more chemisorbed oxygen ions are absorbed on NiO/SnO_2 heterojunction system. Thus more electrons are released back into the conduction band of NiO/SnO_2 composites in H_2 sensing reaction, and lower optimum working temperature and higher gas response are measured for NiO/SnO_2 composites to H_2.

4. Conclusion

A simple and environment-friendly hydrothermal method was employed to prepare pure SnO_2 and NiO-doped SnO_2 nanostructures. The crystalline structures, surface and morphology characteristics, and compositions and chemical states were characterized by XRD, SEM, EDS, and XPS measurement, respectively. Chemical gas sensors were fabricated based on the synthesized samples and their sensing performances to H_2 were performed on a CGS-1TP intelligent gas sensing analysis system. The NiO/SnO_2 composites based sensor demonstrates a lower optimum operating temperature of 325°C and higher gas response than those of pure SnO_2, which could be ascribed to the formation of p-n heterojunctions between p-type NiO and n-type SnO_2. Furthermore, the NiO/SnO_2 composites based sensor exhibits a quasilinear relationship to H_2 gas with concentration ranging 1–50 μL/L. All results indicate that the prepared NiO/SnO_2 composites a promising sensing material for recognition and analysis of dissolved H_2 gas in transformer oil.

Conflict of Interests

The authors declare that there is no conflict of interests regarding the publication of this paper.

Acknowledgment

This work has been supported in part by Fundamental Research Funds for the Central Universities (nos. SWU114051, XDJK2014B031).

References

[1] M. Duval and J. J. Dukarm, "Improving the reliability of transformer gas-in-oil diagnosis," *IEEE Electrical Insulation Magazine*, vol. 21, no. 4, pp. 21–27, 2005.

[2] Q. Zhou, W. Chen, L. Xu, and S. Peng, "Hydrothermal synthesis of various hierarchical ZnO nanostructures and their methane sensing properties," *Sensors*, vol. 13, no. 5, pp. 6171–6182, 2013.

[3] M. Duval, "The duval triangle for load tap changers, non-mineral oils and low temperature faults in transformers," *IEEE Electrical Insulation Magazine*, vol. 24, no. 6, pp. 22–29, 2008.

[4] S. Singh and M. Bandyopadhyay, "Dissolved gas analysis technique for incipient fault diagnosis in power transformers: a bibliographic survey," *IEEE Electrical Insulation Magazine*, vol. 26, no. 6, pp. 41–46, 2010.

[5] W. Chen, Q. Zhou, F. Wan, and T. Gao, "Gas sensing properties and mechanism of Nano-SnO_2-based sensor for hydrogen and carbon monoxide," *Journal of Nanomaterials*, vol. 2012, Article ID 612420, 9 pages, 2012.

[6] W. Zeng, T. Liu, D. Liu, and E. Han, "Hydrogen sensing and mechanism of M-doped SnO_2 (M = Cr^{3+}, Cu^{2+} and Pd^{2+}) nanocomposite," *Sensors and Actuators B: Chemical*, vol. 160, no. 1, pp. 455–462, 2011.

[7] M. Yang, D. H. Kim, W. S. Kim et al., "H2 sensing characteristics of SnO_2 coated single wall carbon nanotube network sensors," *Nanotechnology*, vol. 21, Article ID 215501, 8 pages, 2010.

[8] S. Rumyantsev, G. Liu, R. A. Potyrailo, A. A. Balandin, and M. S. Shur, "Selective sensing of individual gases using graphene devices," *IEEE Sensors Journal*, vol. 13, no. 8, pp. 2818–2822, 2013.

[9] P. Patimisco, S. Borri, A. Sampaolo et al., "A quartz enhanced photo-acoustic gas sensor based on a custom tuning fork and a terahertz quantum cascade laser," *Analyst*, vol. 139, no. 9, pp. 2079–2087, 2014.

[10] C.-H. Han, S.-D. Han, and S. P. Khatkar, "Enhancement of H_2-sensing properties of F-doped SnO_2 sensor by surface modification with SiO_2," *Sensors*, vol. 6, no. 5, pp. 492–502, 2006.

[11] I.-C. Yao, P. Lin, and T.-Y. Tseng, "Hydrogen gas sensors using ZnO-SnO_2 core-shell nanostructure," *Advanced Science Letters*, vol. 3, no. 4, pp. 548–553, 2010.

[12] Z. J. Wang, Z. Y. Li, T. T. Jiang, X. R. Xu, and C. Wang, "Ultrasensitive hydrogen sensor based on Pd^0-Loaded SnO_2 electrospun nanofibers at room temperature," *ACS Applied Materials and Interfaces*, vol. 5, no. 6, pp. 2013–2021, 2013.

[13] W. Wang, Y. Tian, X. Li et al., "Enhanced ethanol sensing properties of Zn-doped SnO_2 porous hollow microspheres," *Applied Surface Science*, vol. 261, pp. 890–895, 2012.

[14] L. He, Y. Jia, F. Meng, M. Li, and J. Liu, "Development of sensors based on CuO-doped SnO_2 hollow spheres for ppb level H_2S gas sensing," *Journal of Materials Science*, vol. 44, no. 16, pp. 4326–4333, 2009.

[15] W. Tang, J. Wang, P. J. Yao, and X. J. Li, "Hollow hierarchical SnO_2-ZnO composite nanofibers with heterostructure based on electrospinning method for detecting methanol," *Sensors and Actuators B: Chemical*, vol. 192, no. 1, pp. 543–549, 2014.

[16] N. van Hieu, P. Thi Hong Van, L. Tien Nhan, N. van Duy, and N. Duc Hoa, "Giant enhancement of H_2S gas response by decorating n-type SnO_2 nanowires with p-type NiO nanoparticles," *Applied Physics Letters*, vol. 101, no. 25, Article ID 253106, 2012.

[17] R. S. Shen, X. P. Li, X. C. Xia et al., "Comparative investigation of three types of ethanol sensor based on NiO-SnO_2 composite nanofibers," *Chinese Science Bulletin*, vol. 57, no. 17, pp. 2087–2093, 2012.

[18] W. Chen, Q. Zhou, and S. Peng, "Hydrothermal synthesis of Pt-, Fe-, and Zn-doped SnO_2 nanospheres and carbon monoxide sensing properties," *Advances in Materials Science and Engineering*, vol. 2013, Article ID 578460, 9 pages, 2013.

[19] Q. Qi, P.-P. Wang, J. Zhao et al., "SnO_2 nanoparticle-coated In_2O_3 nanofibers with improved NH_3 sensing properties," *Sensors and Actuators B: Chemical*, vol. 194, no. 4, pp. 440–446, 2014.

[20] W. Zeng, T. Liu, and Z. Wang, "Enhanced gas sensing properties by SnO_2 nanosphere functionalized TiO_2 nanobelts," *Journal of Materials Chemistry*, vol. 22, no. 8, pp. 3544–3548, 2012.

[21] W. Chen, Q. Zhou, F. Wan, S. Peng, and W. Zeng, "Synthesis and enhanced ethane sensing properties of pt-doped nio nanofibers via electrospinning," *Nanoscience and Nanotechnology Letters*, vol. 5, no. 12, pp. 1231–1236, 2013.

[22] Q. Qi, T. Zhang, X. Zheng et al., "Electrical response of Sm_2O_3-doped SnO_2 to C_2H_2 and effect of humidity interference," *Sensors and Actuators B: Chemical*, vol. 134, no. 1, pp. 36–42, 2008.

[23] Q. Zhou, W. G. Chen, S. D. Peng, and W. Zeng, "Hydrothermal synthesis and acetylene sensing properties of variety low dimensional zinc oxide nanostructures," *The Scientific World Journal*, vol. 2014, Article ID 489170, 8 pages, 2014.

[24] I. Preda, R. J. O. Mossanek, M. Abbate et al., "Surface contributions to the XPS spectra of nanostructured NiO deposited on HOPG," *Surface Science*, vol. 606, no. 17-18, pp. 1426–1430, 2012.

[25] X. Xue, L. Xing, Y. Chen, S. Shi, Y. Wang, and T. Wang, "Synthesis and H_2S sensing properties of CuO-SnO_2 core/shell PN-junction nanorods," *The Journal of Physical Chemistry C*, vol. 112, no. 32, pp. 12157–12160, 2008.